1

Early-Stage Diagnosis of Breast Cancer: Amelioration in Approaches

Nidhi Manhas[1], Lalita S. Kumar[1] and Vinayak Adimule[2]

[1]Indira Gandhi National Open University (IGNOU), School of Sciences, Maidan Garhi, New Delhi, 110068, India
[2]Angadi Institute of Technology and Management, Department of Chemistry, Savgaon road, Belagavi, Karnataka, 590009, India

1.1 Introduction

Breast cancer (BC) has become one of the most prevalent malignant tumors in women and is increasing at an alarming rate. Based on the population growth, experts have predicted that by 2050, there will be roughly 3.2 million new cases per year globally [1]. Not only is the number of patients with BC rising all over the world, but also the age of affected patients is tending to be younger [2]. Many factors contribute to these circumstances including age, family history, lifestyle surroundings, and many others [1, 3, 4]. Although the relative risk of BC is inevitable, it is possible to reduce BC mortality rate. Its survival rate largely depends upon the woman's timely access to effective and affordable detection and treatment processes [5]. The World Health Organization (WHO) has also described two different but related approaches to reduce BC, i.e. *early diagnosis*, which is the recognition of symptomatic cancer at an early stage, and *screening*, which is the identification of asymptomatic disease in a target population of apparently healthy individuals [6]. In many developing countries, women are unaware about the BC because of which it is detected at later stages [7]. However, there are various organizations working for generating awareness and promoting self-examination of the breast among women. Such efforts will promote the early detection and will help in reduction of the BC mortality rate.

Even previous research has shown that early BC detection, if combined with appropriate treatment, could greatly reduce BC death rates in the long run. Therefore, detecting BC at an early stage is vital. There are different techniques used for its diagnosis. Presently, mammography (MG), breast ultrasound, and breast magnetic resonance imaging (MRI) examination are the most common diagnostic techniques available for the detection of BC [8, 9]. These procedures necessitate

Drug and Therapy Development for Triple Negative Breast Cancer, First Edition.
Edited by Pravin Kendrekar, Vinayak Adimule, and Tara Hurst.

specialized equipment, skilled practitioners, and expert analysis but the cost of detection is significantly high. In comparison to these methods, biosensor detection is far more reliable and affordable [10]. Weaver and Leung have summarized the various definitions and applications of biomarkers in imaging BC [11]. On the one hand, breast tumor indicators are critical in the early detection of BC, the characterization of molecular subgroups, the selection of treatment options, and the assessment of survival [12–14], whereas biosensors, on the other hand, provide substantial benefits over standard tumor marker detection methods in terms of specificity, sensitivity, speed, and cost of detection [15, 16] such as chemiluminescence immunoassay [17], enzyme-linked immunosorbent assay [18], proteomics [17], molecular biology methods, and liquid biopsy. Several biosensors with improved sensitivity, selectivity, stability, and low cost have been created in the previous decade [19].

In this chapter, many diagnostic methods such as MG, ultrasonography (US), MRI, microwave BC detection techniques, and various biosensors will be discussed. We herein discuss their most recent advances, as well as their benefits and drawbacks. This will aid researchers and those working on BC diagnostic methods in selecting appropriate approaches for properly diagnosing BC in its early stages.

1.2 Imaging Techniques

The use of imaging techniques reveals the anatomy and position of malignant cells and provides clinicians with valuable clinical information. When contrast agents and high-energy rays are used in imaging procedures, unfortunately, patients may be harmed. As a result, we should discuss different imaging modalities and decide which one is best for BC patients. These techniques mainly include MG, US, MRI, positron emission computed tomography (PET), computed tomography (CT), and single-photon emission computed tomography (SPECT). The benefits and drawbacks of these imaging techniques are listed in Table 1.1.

PET, CT, and SPECT are not advised for diagnosing BC patients due to their high cost, limited practicability, and radiation damage [20]. However, in some circumstances, such as screening for metastatic BC and the presence of bone and lymphatic metastases, these techniques can be employed as additional diagnostic procedures for diagnosing BC. As a result, we solely discuss MG, US, and MRI, which are the primary modalities for detecting BC. These common imaging procedures will be summarized and evaluated to assist clinicians to serve their patients in a better way.

1.2.1 Mammography (MG)

MG is the primary method used for screening and diagnosing BC, and it aids clinicians in gathering clinical data on BC patients. This method is especially advantageous to women between the ages of 40 and 74. Early MG screening may reduce the

Table 1.1 Benefits and drawbacks of imaging techniques.

Imaging techniques	Advantages	Disadvantages
XRM	1) Standard for diagnosing BC patients 2) Suitable as a screening method for BC 3) Finding mammary gland calcification	1) Not for people under 40 2) Not for people with high gland density 3) No more than twice a year
US	1) Screening for young women 2) Noninvasive diagnostic method 3) Finding mammary gland inflammation	1) Not for small mass and a typical tissue 2) Affected by the examining doctor 3) Definition and resolution are not high
MRI	1) High sensitivity and specificity to invasive BC 2) Screening of high-risk groups such as family history of BC 3) For patients with breast-conserving surgery	1) Not for everyone such as patients with claustrophobia 2) Not for wide-scale screening 3) Not for BC staging
PET	1) High sensitivity to BC recurrence and metastasis 2) Helpful for staging of the BC 3) High sensitivity to small breast tumor	1) High cost, not recommended as routine screening 2) Not for patients with hypersensitivity to developer
CT	1) Supplementary diagnostic method for BC, such as identifying BC with or without intrapulmonary metastases	1) Not the first choice for diagnosing BC 2) Radiation damage 3) Poor spatial resolution and need experienced doctors
SPECT	1) High resolution, small field of vision 2) Recommended use when suspects metastasis	1) Obtaining little clinic information 2) Not for patients with inflammatory bone lesions and bone proliferative metabolic abnormalities or variations

CT, computed technology, MRI, magnetic resonance imaging, PET, positron emission tomography, SPECT, single-photon emission computed tomography, US, ultrasonography, XRM, X-ray mammography.

death rate of BC patients by 30% to 40%, according to one of the earlier research [21]. However, MG has a significant rate of false-positive and false-negative results, especially in individuals with dense breasts (for subjects under 40 years old) [22, 23]. But with time, MG is progressing continuously and has shown good results in terms of diagnostic accuracy, sensitivity, and resolution. Presently, two key diagnostic methods are under practice for detection, i.e. contrast-enhanced mammography (CEM) and digital breast tomosynthesis (DBT) [24, 25]. CEM has been found to be superior

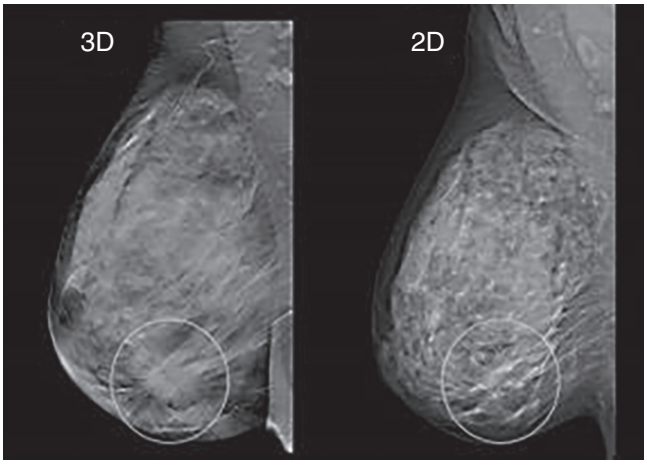

Figure 1.1 3D versus 2D mammography. Source: Andersson et al. [33]/Reproduced with permission from Springer Nature.

to full-field digital mammography (FFDM) in terms of diagnostic accuracy and disease extent assessment, and its efficiency is also comparable to that of MRI as well as US [26–28]. When compared to FFDM, DBT also offers good performance in terms of specificity (96.4%, 57 229/59 381% versus 97.5%, 23 427/24 020, $P < 0.001$) [29]. Computer-aided detection (CAD) is an artificial intelligence (AI) technique that has improved the sensitivity of the instrument and decreased human errors as well as false-positive and false-negative results in detection [30]. The combination of CAD with CEM and DBT can significantly improve the performance of these imaging techniques [31, 32]. In individuals who have no indications or symptoms of BC, a 3D MG is utilized to detect the disease as shown in Figure 1.1. The study demonstrated that combining 3D and traditional MG minimizes the need for extra imaging and has increased the accuracy of MVGG up to 94.3% [34]. Various algorithms have been proposed to enhance the MG images. After many experiments and selecting suitable settings, Montaha et al. suggested the BreastNet18 model, which is based on the fine-tuned VGG16. The accuracy of the algorithm grew to 98.02% of the proposed model [35]. Such type of research will help the doctors in efficient and accurate diagnosis of BC.

From the above discussion, we can conclude that MG is an essential component of early diagnosis for BC patients because of its several benefits, including rapid screening, high accuracy, low cost, and suitability for promoted use. Despite these benefits, MG is not suitable for everyone. It requires a hazardous contrast agent and X-ray to perform imaging, cannot be used frequently in a short period of time, and is not suggested for people under the age of 40 [36]. But in the coming years, with significant developments like high resolution, MG will be quite safe. Moreover, advances in AI technology have made it possible to simplify the detection and analysis of BC.

1.2.2 Ultrasonography (US)

US is a technique for evaluating the form and status of tumor tissues, as well as correctly locating lesions. The early grayscale US merely showed whether the tumor existed at the detecting point, and because its resolution was inadequate, it was difficult to discriminate benign and malignant tumors [37, 38]. US images showing normal, benign, and malignant BC are given in Figure 1.2.

The flat photographs of tumors received from the two-dimensional (2D) US might affect the physician's assessment. Therefore, three-dimensional (3D) US technology was introduced so that one can have 3D imaging of tumor anatomy and blood vessel distribution in diagnosed patients [40]. The color **Doppler ultrasound** is one of the 3D techniques of ultrasounds that may vividly display tumor and blood flow information and offer clinicians more useful information, allowing them to discriminate between malignant and benign tumors [41]. Krouskop discovered elastic variations in different tissues laying the theoretical groundwork for constructing elastic US [42]. Furthermore, some studies revealed that employing elastic US to screen suspected diseased tissues considerably enhances the accuracy of diagnosing BC [43, 44]. The elastic US, when paired with 3D US, can diagnose axillary lymphadenopathy and classify the patient's tumor state [45]. Although MG is the best tool for detecting BC calcification, when the calcification is too tiny, it is difficult to identify with MG or normal US; so, **MicroPure**, a new US image-processing method, was developed [46]. By analyzing images of multidimensional array and frequency, this method may decrease random noise and produce high-resolution images and tissue homogeneity [47]. Machado et al. examined *ex vivo* surgical breast specimens with MicroPure and discovered that MicroPure has a high detection rate for BC microcalcifications, whereas conventional US cannot detect [48].

This technique has significant advantages that include the use of less contrast agents, the absence of high-energy rays, and the fact that it is suited for people of all ages. US has been suggested as a supplement to MG for women at high risk of BC, pregnant women, and those who are unable to get MG [49]. Furthermore, it involves the use of skilled radiologists, which has a major impact on sensitivity and specificity. Breast ultrasound has a high false-positive rate while being routinely shown to detect mammographically hidden malignancies. However, using AI, radiologists

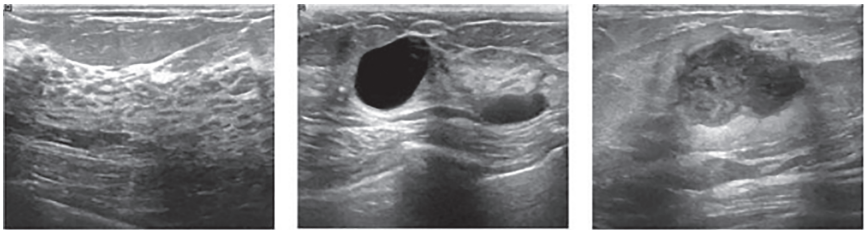

Figure 1.2 Samples of ultrasonography breast images dataset. Source: Dhabyani et al. [39]/with permission from Elsevier/CC BY 4.0.

were able to cut false positive rates by 37.3% and requested biopsies by 27.8% while retaining the same sensitivity level (Area Under the Receiver Operating Characteristic Curve [AUROC]: 0.962 AI, 0.924 ± 0.02 radiologists) [50]. AI has the potential to improve the accuracy, consistency, and efficiency of breast ultrasound diagnosis in the future, which will help doctors achieve more accurate diagnostic results by reducing errors caused by unprofessional judgments.

1.2.3 Magnetic Resonance Imaging (MRI)

MRI enables the early diagnosis of BC, independent of the patient's age, breast density, or risk status [51]. The common approach for breast imaging is dynamic contrast-enhanced magnetic resonance imaging (DCE-MRI), which focuses on the introduction of contrast agents and displays the malignant vascularity, anatomy, and kinetics of breast tumors [52]. DCE-MRI has been demonstrated as a screening technique for women with a variety of risk levels, with sensitivity ranging from 81% to 100% [53]. The positive prognostic value of DCE-MRI is 98%, which is higher than the positive prognostic value of MRI alone, i.e. 77% and the specificity is 97%, according to the experts [54]. Another recently developed method that allows for excellent spatial and temporal resolution is ultrafast DCE-MRI in which various amplification approaches, such as parallel imaging and compressed sensing, are applied, and its ability to characterize BC aggressiveness and tumor subtypes has been proven [55]. There is another technique called **Magnetic Resonance Diffusion Weighted** (MRDW). It is also used in BC diagnosis that shows clear movement of water molecules in the body, as for different tissues there exist different water dispersion coefficients. Researchers can detect benign and malignant breast tumors by utilizing MRDW to evaluate apparent diffusion coefficient (ADC) values (which reflect diffusion-limited effects) of tumors, i.e. ADC values: normal breast group > benign group > malignant group [56, 57]. DWI has the advantage of being a non-contrast technology with a fast scan time [58]. Moreover, DWI was found to be more accurate than MG in detecting cancer in a sample of asymptomatic women [59].

Magnetic resonance spectroscopy (MRS) is an important method that is used to describe the functional state of malignant, benign, and normal breast tissues in three ways: *in vivo*, *ex vivo*, and *in vitro*. Table 1.2 compares the studies of *in vitro*, *ex vivo*, and *in vivo* MRS and MRI techniques in the diagnosis of BC [60]. MRS is a noninvasive technology that can enhance the rate of BC diagnosis by assessing the risk of BC and leading to BC treatment [61, 62]. Solid-state MR spectroscopic examination of intact biopsied tissues employing the high-resolution magic angle spinning (HRMAS) approach was also employed in studies to monitor metabolite levels for breast tumor diagnosis/prognosis [63–68]. High amounts of choline-containing metabolites (tCho) were found in breast *in vivo* MRS experiments, indicating the rapid proliferation of malignant tumors [69–76]. Hyperpolarized ^{13}C MRI (HP ^{13}C MRI) has recently been used to investigate abnormal tumor metabolism [77].

Table 1.2 Comparison of *in vitro*, *ex vivo,* and *in vivo* magnetic resonance spectroscopy (MRS) and MRI techniques.

	Magnetic resonance spectroscopy (MRS)			
Characteristics	***In vitro***	***Ex vivo***	***In vivo***	**MRI**
Information	Biochemical composition (metabolite detection)	Biochemical composition (metabolite detection)	Biochemical composition (metabolite detection)	Anatomy (structure and morphology), functional
Sample/subject	Tissue extract, biofluids, cell lines, aspirates	Excised tissues/biopsies	Living humans/organisms	Living humans/organisms
Equipment	NMR spectrometer	NMR spectrometer with accessories for HRMAS	Human MRI scanner	Human MRI scanner
Field strength	High field strength 9.4–21.1 T	High field strength 9.4–18.8 T	1.5–7T	1.5–7T
Nuclei of interest	^{1}H, ^{13}C, ^{31}P, ^{23}Na, ^{19}F	^{1}H, ^{13}C	^{1}H, ^{31}P, ^{23}Na, ^{19}F ^{13}C hyperpolarized	^{1}H from fat and water
Data	1D/2D spectra	1D/2D spectra	SVS 1D, SVS-2D, CSI (MRSI)	Conventional T1, T2-weighted, DCE-MRI, diffusion-weighted, perfusion weighted, MR elastography, fMRI
Advantages	High sensitivity and resolution, detection of a large number of metabolites, easy quantification, easy experimentation	High sensitivity and resolution, detection of a large number of metabolites, quantification not that easy, special experimentation	Organ-specific metabolite composition, and longitudinal studies	Organ-specific structural and functional studies, longitudinal studies possible
Limitations	Tissue excision is invasive	Tissue excision is invasive	Low sensitivity and resolution, detection of a small number of metabolites, claustrophobia of patients	Claustrophobia of patients contrast required in some studies
Reproducibility	Lesser than *in vivo*	Lesser than *in vivo*	High	High

1D, one-dimensional spectrum; 2D, two-dimensional spectrum; HRMAS, high-resolution magic angle spinning; SVS, single voxel spectroscopy; CSI, chemical shift imaging; DCE-MRI, dynamic contrast-enhanced magnetic resonance imaging.

Source: Sharma and Jagannathan [60] ©MDPI/Public Domain CC BY 4.0.

Magnetic resonance elastography (MRE) is a type of magnetic resonance technology that uses the transmission of mechanical waves in tissues to offer information on tissue elasticity. MRE's future tendency is to identify preoperative tumors and predict treatment response and metastatic potential of primary tumors [78]. PET/MRI or PET and MRI can reveal soft tissue structures in the breast and chest wall. PET can offer molecular-level information *in vivo*, and PET/MRI has a high value in evaluating BC metastasis and can improve the positive predictive rate of patients [6, 79, 80]. Moreover, AI-enhanced model of ^{18}F-FDG PET/MRI (^{18}F-fluorodeoxyglucose positron emission tomography magnetic resonance imaging) has accurately shown the difference between benign and malignant breast lesions [81].

MRI is a supplementary method for diagnosing BC that seems to have a number of advantages. Unfortunately, numerous factors influence the widespread use of MRI, i.e. prolonged imaging time, high price, and the fact that it cannot be performed if the patient's body contains metal material. As a result, future research should focus on lowering the cost of MR procedures and reducing the need for contrast agents, so that they can be used at early stages of the BC. Radiomics is a fast-developing area that uses AI algorithms to analyze medical scans digitally, allowing for thorough tumor characterization [82–84]. So, radiomics applications should be thoroughly investigated, and there is a need to improve radiologists' grasp of basic principles and the development of standardized and reproducible methods and data exchange for clinical applications.

1.3 Microwave Breast Imaging Methods

The microwave region ranging between 300 MHz and 300 GHz has received the least attention but has sparked a lot of interest in medical imaging in the last two decades. In this, the interaction of electromagnetic signals with the matter is determined by the dielectric properties of the matter, i.e. electric permittivity and conductivity [85]. Microwave imaging (MWI) has evolved as a technology for creating dielectric maps of various body sections. Basically, a MWI system includes an antenna array, a microwave signal transmitter and receiver, and a radio-frequency switch to switch between the arrays' multiple parts [86]. There are some applications of MWI in brain stroke detection [87], extremity imaging [88, 89], and lung cancer detection [90]. However, in this chapter, we have mainly discussed its application in BC detection. Tumors have high water content when compared to normal cells. This is due to the biology of tumor cells, which retain more fluid than normal cells. The dielectric characteristics of breast tissues are altered by this additional fluid, which is in the form of bound water. Tumors are diagnosed by MWI using scattered or reflected waves emerged from variations in dielectric characteristics between normal and malignant breast tissues [91–93]. Table 1.3 shows the difference in the dielectric properties of the female breast tissue at 3.2 GHz [94].

Table 1.3 Dielectric properties of female breast tissue at 3.2 GHz.

Tissue type	Relative permittivity	Conductivity (mS cm^{-1})	Water content (%)
Fatty tissue	2.8–7.6	0.5–2.9	11–31
Normal tissue	9.8–46	3.7–34	41–76
Benign tissue	15–67	7–49	62–84
Malignant tissue	9–59	2–34	66–79

Source: Adapted from Campbell and Land [94].

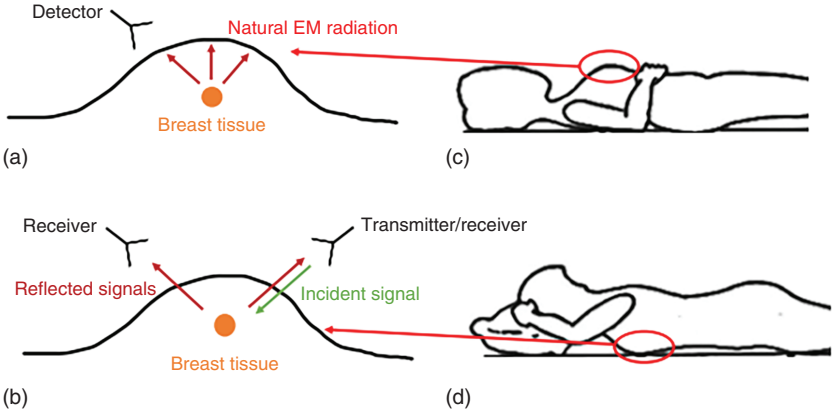

Figure 1.3 Methods of microwave breast imaging. The figures on the left show (a) passive versus (b) active approaches. The figures on the right show patient's orientations for (c) planar systems (supine position) versus (d) cylindrical systems (prone position). Source: AlSawaftah et al. [85] ©MDPI/Public Domain CC BY 4.0.

The MWI techniques can be classified into two groups, active MWI and passive MWI. The active MWI techniques are further subcategorized into microwave tomography (MWT) and radar-based MWI. Active MWI examines the difference in dielectric properties between the healthy and malignant tissues, and passive MWI measures the temperature between the healthy and cancerous tissues using radiometry [95]. The primary distinction between these two approaches is that natural electromagnetic radiation released by living tissues is measured in passive systems, whereas in active systems, an electromagnetic signal from a source is incident on the tissues and the reflected signals are measured (as depicted in Figure 1.3) [85].

1.3.1 Microwave Tomography

MWT is a technique that uses electromagnetic field alterations to obtain 2D slices or pictures of the dielectric characteristics of a sample. Typically, MWT setup includes imaging chamber, which is filled with the matching medium, and to improve the

performance of this system matching medium, is selected carefully so that most of the microwave electromagnetic signals can couple with breast tissue. Imaging chamber also has array of antennas surrounding the sample, where each antenna transmits a continuous wave (CW) of single- or multifrequency electromagnetic signals. The electromagnetic signals scattered by matching medium and sample because of differences in their dielectric properties are measured by non-transmitting antennas. After analyzing data using algorithms, 2D images of dielectric properties are created. So, we can say that there are basically three steps to create image, i.e. collecting microwave tomogram, data analyzing, and then image display using MWT [85].

Several theoretical and experimental research studies have been done on the use of this method in BC diagnosis [96–100]. Meaney et al. [99] have done series of experiments to improve the performance of this technique. First multifrequency MWT prototype for breast imaging was set up of a cylindrical array of 16 monopole antennas operating at 300–1000 MHz [96]. This study revealed the relationship between the breast permittivity and radiological breast density. Another experiment with glycerin and water mixture as matching medium was done and found that it helped in the reduction of coupling noises between array elements. The results of these clinical investigations showed that tumors as small as 1 cm in diameter can be diagnosed, indicating that MWT has the ability to detect early-stage BC [101–103].

In recent research, magnetic nanoparticles and compressive sensing (CS) techniques are used as contrast agents to improve the accuracy, sensitivity, and specificity of MWT in BC detection [104, 105]. The results showed that the CS-based MWT with 12 antennas and an MWT with 70 antennas provided equal-quality breast pictures. Thus, we can conclude that CS-based MWT technique lowered operation costs and data-gathering time significantly.

1.3.2 Radio-Based Microwave Imaging

During BC detection, a radio-based MWI technology exploits reflected waves caused by differences in dielectric characteristics between normal and malignant tumor cells and gives valuable information about the location, size, and characteristics of tumor cells. First radar-based MW system was proposed by Bridge [106]. In Bridge's method, ultrawideband (UWB) of microwave frequency ranging from 1 to 10 GHz was used to illuminate BC tissue from array of antennas placed at different positions around the breast [107, 108]. Radar-based MW has more advantages over MWT such as being computationally less expensive, having higher resolution, and having better specificity [108, 109].

As per the developments in radar-based MW, it is classified into five groups [95]:

- **Confocal microwave imaging (**CMI**)**: Hagness et al., first proposed this approach and used pulsed confocal techniques with time gating to improve tumor identification while decreasing tissue asymmetry and absorption effects [110]. Their work involves finite-difference time-domain (FDTD), and its results showed that cancer cells having 2 mm diameter can be detected by the 2D CMI.

By utilizing a resistive bowtie antenna and using 3D-FDTD simulations, Hagness et al. improved the prior design [111]. This technique has the potential to produce high-resolution images, but its limitation is that it can't distinguish between errors and noise.

- **Multi-static adaptive (**MSA**) system**: The high-impact radar-based MWI system was developed in which real aperture array of UWM antennas was used. It consisted of 16 UWB aperture-coupled stacked-patch antennas located on the section of hemisphere that were arranged in such a way as to improve the conformation to the curve of the breast [112–114]. The results of the clinical trials showed that this system was successful in detecting the 4–6 mm diameter of cancerous cells [113]. The Breast Care Center in Bristol, UK, conducted a substantial initial trial of the group's 31-element prototype radar system in 2010. Despite the fact that this technique produced good results, the clinical trial findings were mixed. The results were shown to be irreproducible when performed by different clinicians. This is due to slight patient movements throughout the 90-second scans, as well as certain ambiguities caused by changes in blood flow and temperature. In order to resolve these flaws, the team developed a 60-antenna array system to improve the system's immunity to clutter and reduce the scan time to 10 seconds. The results showed increase in the accuracy of the images obtained while also delivering a more convenient and acceptable clinical experience for patients [85].
- **Tissue-sensing adaptive radar (**TSAR**)**: Fear et al. investigated the use of TSAR in BC imaging [115, 116]. This system required the use of two scans of each breast. The first scan specifies the basic location of the breast volume relative to the tank (containing coupling fluid and antennas) obtained at the antenna after the first reflection. The second scan is done in a sagittal direction, from the nipple to the chest wall, providing data for the tumor detection algorithm [116]. The results of these clinical experiments showed that TSAR has the potential to detect and localize tumor with more than 4 mm in diameter [117]. However, the huge reflections created by skin, the construction of adequate antennas, and the desire to develop high-speed electronics for real-time photography all posed hurdles to this system. Development of appropriate sensors, research of practical implementation challenges, enhancement of imaging algorithms, and testing on breast models are all part of the current work on TSAR [95, 118].
- **Microwave imaging via space–time (**MIST**) beamforming**: This type of technique involves the use of continuous transmission of UWB signals from antenna placed near the breast surface, and the received reflected signals are spatially focused using a space–time beam former. Because of the considerable difference in the dielectric characteristics of normal and malignant tissue, discrete regions of high backscattered energy levels appear in the reconstructed pictures, corresponding to malignant tumors [119]. The first MIST system was introduced by Bond et al. [119], resulting in the detection and localization of very small synthetic tumors embedded in breast phantoms [119]. Bond et al. also developed a MIST system with implementation of a planar array of 16 horn antennas that

transmitted UWB microwave signals from each antenna located close to the breast surface [119]. This has resulted in significant improvement in the performance of the UWB-based MI approach. However, further improvements enabled the system to localize, identify, and resolve multiple tumors [118, 119].

- **Holographic microwave imaging (**HMI**)**: HMI has the ability to provide real-time images at a substantially cheaper cost than other radar-based MWI approaches since it does not require expensive ultra-high-speed electronics. In this approach, MWI is performed in two stages: recording of a sampled intensity pattern followed by image reconstruction [120]. Smith and coworkers presented a near-field indirect HMI approach that involves capturing the breast intensity and reconstructing the image from that data [120, 121]. However, before this technique can be used in clinical settings, it needs to be validated further.

Wang et al. proposed far-field HMI in which 3D HMI image was reconstructed using 2D HMI images obtained at different vertical positions with single frequency (12.6 GHz) for early detection of BC [122]. It included one transmitter and an array of 15 receivers placed under the breast phantom. In this system, matching solution medium is not required and air between the antennas and breast phantom. The results of the experiments demonstrated that the suggested 2D HMIA approach could successfully detect tiny tumors with a diameter of less than 5 mm in various places [122]. The other experiment was done by combining the above approach with CS, and results showed that CS-HMIA has the capability of detecting randomly distributed inclusion of various shapes and sizes using smaller number of sensors and lesser scan times [123]. In a recent development, a multifrequency HMI system has been developed by Wang (2019), who checked the feasibility and effectiveness of the proposed algorithm for breast imaging [124]. According to the studies, the multifrequency HMI system has the ability to be used as a microwave diagnostic technology.

A significant amount of research and development is yet to be done in harnessing the full potential of this technology. The future research should focus on improvement of MWI in medical applications, including better designing of hardware, signal processing methods as well as algorithms for image reconstruction.

1.4 Biomarkers and Biosensors for Breast Cancer Detection

The molecular biotechnology studies are done to analyze specific biomarkers such as nucleic acids, proteins, cells, and tissues of patients, and these studies help in early detection of BC than abovementioned imaging techniques or procedures [20]. However, these cannot replace imaging techniques but can be used as auxiliary method to diagnose BC. The examinations help the clinician analyze BC from the level of nucleic acids, proteins, and cells using these biomarkers and biosensors. First, we will discuss biomarkers and then biosensors.

1.4.1 Biomarkers

1.4.1.1 Nucleic Acids

There are different nucleic acid tumor markers viz, BRCA1, BRCA2, microRNA, circulating tumor DNA (ctDNA), circulating cell-free DNA (ccfDNA), circulating RNA (circRNA), long noncoding RNAs (lncRNAs), etc. [125]. MicroRNA is a single-stranded noncoding RNA molecule that has evolved as a significant regulator of BC development, prognosis, and therapeutic response [126]. The study has revealed that MicroRNA has been linked to patients' clinical and biological characteristics and that it can target different genes and alter different pathways. LncRNA is a type of noncoding RNA with a length greater than 200 nt that is produced by RNA polymerase II. The role of lncRNAs in the initiation, development, and metastasis of BC is becoming clearer, and they could represent a new diagnostic marker and therapeutic target for BC [127]. CircRNA is a type of double-stranded closed RNA that is resistant to RNA exonuclease, exhibits steady expression, and is difficult to disintegrate according to the findings, CircRNA expression was linked to tumor cell proliferation, migration, invasion, and treatment resistance [128, 129]. Thus, it can be explored as diagnostic method.

ccfDNA is extracellular DNA found in plasma or serum, and ctDNA is ccfDNA released into the bloodstream by tumor cells [130, 131]. The studies have revealed that primary tumor cells, circulating tumor cells, and hidden and dominant metastatic tumor cells all release more DNA than normal cells, and ctDNA contains mutations that are exclusive to the parent tumor [132]. As a result, ctDNA has the potential to be used as a tumor marker for BC prediction, diagnosis, and prognosis [131, 133]. However, further research is needed to apply it to clinical diagnosis and treatment [133].

1.4.1.2 Proteins

CD24, CD44, and MUC1 are some types of protein tumor biomarkers. CD24 is a glycosylphosphatidylinositol-binding glycoprotein [12, 134], which has been discovered to be an anti-phagocytic signal that protects cancer cells from Siglec-10-expressing macrophage attacks. The expression of CD24 has also been linked to BC grading and staging [135]. As a result, CD24-blocking therapy can significantly improve the therapeutic impact of CD24-positive cancers [134]. On the other hand, CD44 is a complex transmembrane-binding glycoprotein that has been linked to a poor prognosis in patients. It is involved in the regulation of numerous critical signaling pathways, including tumor growth, invasion, metastasis, and treatment resistance [135–137].

MUC1 (CA15-3) is a transmembrane mucin glycoprotein that is found in the majority of epithelial tissues [138]. It was shown to have aberrant profile and glycosylation in 90% of BC cases [139]. MUC1 is also a useful marker for tracking the progression of metastatic BC [140]. Further, serum tumor markers such as CEA, CA19-9, CA125, CA15-3, and TPS play a significant role in the diagnosis and treatment of BC [141].

1.4.1.3 Tumor Cells

The term "circulating tumor cells (CTCs)" refers to BC cells that have broken free from the tumor and entered the bloodstream (CTC). CTCs have the ability to regenerate tumor tissue. So such types of tumor cells themselves are tumor markers [141]. Patients with metastatic BC could be tiered and graded to get tailored treatment by measuring the number of CTC cells [142]. CTC cells can also be used to assess BC patients' prognoses and identify whether they are candidates for further radiation therapy after surgery [132, 143].

Apart from nucleic acid, proteins, and tumor cells, exosomes (membrane-enclosed phospholipid extracellular vesicles) can also be applied in the diagnosis and treatment of cancer due to their high secretion on the surface of cancer cells [144]. From the research findings, it was shown that tumor cells release more exosomes than normal cells, and miRNA-21 and miRNA-1246 in exosomes are upregulated in patients' plasma [9]. Therefore, exosomes have become a research hotspot in recent years because of their great diagnostic potential. In addition to exosomes, estrogen receptor (ER) [145], progesterone receptor (PR) [146], and human epidermal growth receptor 2 (HER2) [147] are the most widely used tumor markers in the early diagnosis and treatment of BC. The diagnosis of BC using tumor markers with high specificity and sensitivity requires more research.

1.4.2 Biosensors

A biosensor is a self-contained, tiny analytical instrument that combines a specific biological system with a physiochemical transducer to detect target molecules by transforming the recognition signal into a detectable output signal [148–152]. When compared to traditional tumor marker detection methods, biosensors offer substantial advantages in terms of specificity, sensitivity, speed, and cost of detection [15, 16]. Biosensors can be divided into electrochemical biosensors, optical biosensors, and other types on the basis of detection principles and signals [19, 151–154].

1.4.2.1 Electrochemical Biosensors

Electrochemical biosensors monitor changes in dielectric characteristics, size, shape, and charge distribution when antibody–antigen complexes form on the electrode surface. By sensing the electrochemical reaction on the electrode's surface, it quantitatively detects the analyte and the signal of the electrochemical reaction, which depends on the concentration of analyte [155–157]. These biosensors have been designed to detect a variety of biomolecules, including proteins, antigens, DNA, antibodies, and heavy metal ions, among others. Electrochemical sensors have previously been shown to have great sensitivity and specificity in buffer and serum samples [158]. Figure 1.4 shows the developed electrochemical biosensor for MCF-7 cells detection [160]. Antibodies against surface proteins of MCF-7 cells were immobilized on nanoparticle-assembled electrode to capture MCF-7 cells at the electrode surface, which increases the interfacial resistance and hence enlarged semicircle in Nyquist plot. Alternatively, cDNA complementary to miRNA can also be immobilized to capture target miRNA released from the cell extracts of MCF-7 cells [95].

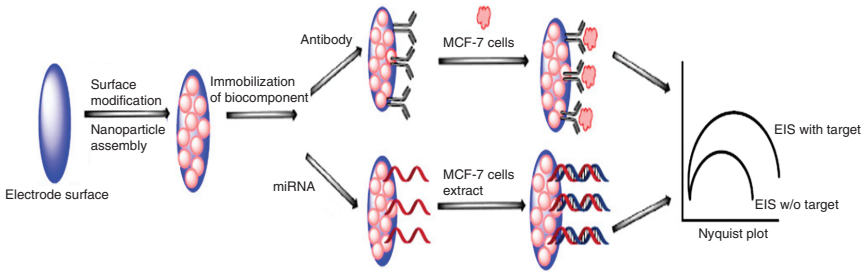

Figure 1.4 Electrochemical biosensor for detection of MCF-7 cells. Source: Mittal et al. [159]/with permission of Elsevier.

There are some methods through which the detection of electrochemical reaction is done: cyclic voltammetry (CV), differential pulse voltammetry (DPV), square wave voltammetry (SWV), linear sweep voltammetry (LSV), electrochemical impedance spectroscopy (EIS), field-effect transistor (FET), and other methods [19, 148, 149] as shown in Table 1.4. Recent development of electrochemical nanobiosensors has reduced the cost, simplified the technique, increased sensitivity and specificity, increased reliability, and provided a quick response in BC detection [178, 179]. Further research in this direction would be helpful in early detection of BC.

1.4.2.2 Optical Sensors

Optical biosensors detect the optical change on the surface of sensing layer of the target. Every optical biosensor detects different optical signals such as refractive index, resonance, wavelength, and intensity [16, 180, 181]. As shown in Figure 1.5, the diagnosis of BC cell (MCF-7) is done using quantum dot optical biosensor. In Figure 1.5, quantum dots are labeled with primary antibodies against MCF-7 cell surface proteins and subjected to sample containing MCF-7 cells. Addition of secondary antibody labeled, magnetic beads enables sensors for their magnetic separation to obtain fluorescence emission spectra [95]. Different types of optical biosensors have been developed that include fiber optics, fluorescence, resonant mirror optical, interferometric, and surface plasmon resonance as given in Table 1.5. Recently, these sensors have been developed using surface chemistry and nanotechnology [194].

In addition to electrochemical and optical biosensors, there are two other types of sensors viz, quartz crystal microbalance (QCM) biosensors (which detect mass change of the target) and photoelectochemical (PEC) biosensors (which detect the effect of the targets on the photoelectric characteristics of materials).

- **QCM biosensor**: The effect of the target on the frequencies of the bulk acoustic waves generated in the piezoelectric quartz crystal is the basis for QCM's sensing mechanism. To achieve the concentration detection of the target, the frequency change of the acoustic wave is connected to the mass change on the chip surface. QCM can detect mass changes on the chip surface at the nanogram level [195].
- **PEC biosensors**: The photoelectric active material in the PEC sensor is stimulated when light is irradiated, resulting in a photocurrent or photovoltage. The target is captured by the recognition sensor on the surface of the photoelectrically

Table 1.4 Developments in electrochemical biosensors.

Electro-chemical biosensor	Target	Detection limit	Linear range	References
CV	CA15	30.64 U ml^{-1}	2.0–240 U ml^{-1}	[161]
	EGFR	1 pg ml^{-1}	1 pg ml^{-1} to 100 ng ml^{-1}	[162]
	miRNA	155.2×10^{-20} M	2×10^{-20} to 2×10^{-12} M	[163]
DPV	BRCA1 CA15-3	0.0034 pM	0.01 pM to 1 nM	[164]
	BRCA1	3.34 mU ml^{-1}	0.01–1000 U ml^{-1}	[165]
	miRNA	3.01×10^{-16} M	1.0×10^{-15} to 1.0×10^{-7} M	[166]
		3.6 fM	0.01–10 pM	[167]
		8.2 fM (miRNA-21)	0.02–10 pM (miRNA-21)	
SWV	MUC1	0.33 pM	1.0 pM to 10 μM	[168]
	miRNA-21	18.9 aM (miRNA-21)	—	—
	miRNA-155	39.6 aM (miRNA-155)	0.1 fM to 10 nM	[169]
LCV	HER2-ECD	4.4 ng ml^{-1}	15–100 ng ml^{-1}	[170]
	HER2	0.16 ng ml^{-1}	7.5–50 ng ml^{-1}	[171]
	CD44	2.17 pg ml^{-1}	0.01–100 ng ml^{-1}	—
	CD44 positive cell	8 cells ml^{-1}	10–106 cells ml^{-1}	[172]
EIS	HER2	19 fg ml^{-1}	0.001–10 ng ml^{-1}	[173]
	MCF-7 cell MUC1	23 cells ml^{-1}	1×10^{2} to 1×10^{5} cells ml^{-1}	—
	BRCA1	2.7 nM	5–115 nM	[174]
		3 fM	10 fM to 0.1 μM	[175]
FET	miRNA-155	0.03 fM	0.1 fM to 10 nM	[176]
	CEA	10 pg ml^{-1}	0.1–100 ng ml^{-1}	[177]

Source: Adapted from Hong et al. [141].

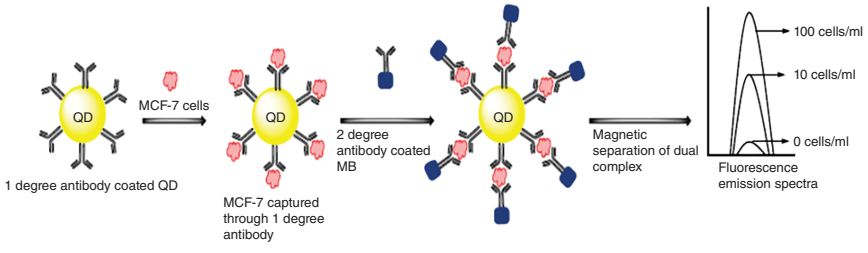

Figure 1.5 Quantum dot based optical biosensor for detection of MCF-7 cells. Source: Mittal et al. [159]/with permission of Elsevier.

active material, causing the photocurrent or photovoltage to change. When the target's concentration changes, so does the photoelectric signal. Therefore, it sets up relationship between the photoelectric signal and concentration. The detection of tumor markers has been reported using several PEC biosensors [141].

Table 1.5 Developments in optical biosensors.

Optical biosensor	Target	Detection limit	Linear range	References
Fluorescence biosensor	CEA	7.9 pg ml^{-1} (Water) 10.7 pg ml^{-1} (human serum samples)	0.03–6 ng ml^{-1} (water) 0.03–6 ng ml^{-1} (human serum samples)	[182]
	miRNA-21	0.03 fM	0.1–125 fM	[183]
Colorimetric biosensor	BRCA1	10^{-18} M	10^{-12} to 10^{-18} M	[184]
	BRCA1	0.34 fM	1 fM to 100 pM	[185]
SPRi	CEA	0.12 ng ml^{-1}	0.40–20 ng ml^{-1}	[186]
	HER2-positive	8280 exosomes μl^{-1}	8280–33 100 exosomes μl^{-1}	[187]
	EXO	5000 exosomes ml^{-1}	—	[188]
	EXO			
SERS	miR-K12-5-5p	884 pM	—	[189]
	MicroRNA	—	—	[190]
ECL	BRCA1	0.71 fM	1.0 fM to 0.1 nM	[191]
	EXO	7.41 × 104 exosomes	3.4×10^5 to 1.7×10^8 exosomes ml^{-1}	[192]
	miRNA-21	3.2 fM	0.01–10 000 fM	[193]

Source: Adapted from Hong et al. [141].

Both of these are also capable of detecting all types of tumor markers. However, they have trouble identifying multiple targets at the same time, but signal amplification techniques can be used to enhance their detection limits for detecting a single target. The obstacles that biosensors have experienced are mostly due to two factors: detection method and detection equipment. These issues can be overcome by the combination of molecularly imprinted polymers (MIPs) and microfluidic chips with biosensors, and the commercialization of these types of biosensors in the future can change the current trend of diagnosis [196, 197].

1.5 Conclusion

This chapter mainly focused on the most frequent approaches for diagnosing BC. As researchers delve more into imaging technology, they know that a single imaging method is just not enough to meet the requirement of accuracy in BC diagnosis. Thus, combining many imaging modalities will be significant for the emerging approaches [107, 198, 199]. Moreover, developments of AI-based models will help in improving the positive diagnostic rate for BC and reducing the negative diagnosis rate. Additionally, the development of biosensors would lead to the formation of various BC biomarkers. The combination of imaging sensors and biosensors can get unexpected results. Nevertheless, imaging instruments would still be the routine method for screening BC over the next few years as these can be widely applied.

The new BC markers will enable these technologies to achieve more efficiency, speed, sensitivity, and specificity. With the development and application of these approaches in the future, the researchers will be able to not only diagnose BC from multiple perspectives but also monitor the effectiveness of treating BC.

Acknowledgment

All the authors are thankful to the School of Sciences, IGNOU, for their continuous support in using the literature resources.

Conflict of Interest

The authors have no conflict of interest.

Authors Contribution

Dr. Vinayak Adimule conceived the idea; Dr. Lalita S. Kumar and Nidhi Manhas wrote the manuscript. All the authors reviewed the manuscript.

References

1 Tao, Z.Q., Shi, A., Lu, C. et al. (2015). Breast cancer: epidemiology and etiology. *Cell Biochem. Biophys.* 72 (2): 333–338.
2 DeSantis, C.E., Ma, J., and Jemal, A. (2019). Trends in stage at diagnosis for young breast cancer patients in the United States. *Breast Cancer Res. Treat.* 173 (3): 743–747.
3 McPherson, K., Steel, C.M., and Dixon, J.M. (2000). ABC of breast diseases: breast cancer–epidemiology, risk factors, and genetics. *BMJ* 321 (7261): 624–628.
4 Zografos, G.C., Panou, M., and Panou, N. (2004). Common risk factors of breast and ovarian cancer: recent view. *Int. J. Gynecol. Cancer* 14 (5): 721–740.
5 Ginsburg, O., Yip, C.H., Brooks, A. et al. (2020). Breast cancer early detection: a phased approach to implementation. *Cancer* 126: 2379–2393.
6 World Health Organization (WHO) (2017). WHO guide to cancer early diagnosis. WHO. http://www.who.int/iris/handle/10665/254500 (accessed 12 April 2020).
7 Yip, C.H. (2016). Challenges in the early detection of breast cancer in resource-poor settings. *Breast Cancer Manag.* 5: 161–169.
8 Pace, L.E. and Keating, N.L. (2014). A systematic assessment of benefits and risks to guide breast cancer screening decisions. *JAMA* 311: 1327–1335.
9 Jafari, S.H., Saadatpour, Z., Salmaninejad, A. et al. (2018). Breast cancer diagnosis: imaging techniques and biochemical markers. *J. Cell. Physiol.* 233 (7): 5200–5213.

10 Panesar, S. and Neethirajan, S. (2016). Microfluidics: rapid diagnosis for breast cancer. *Nanomicro Lett.* 8: 204–220.

11 Weaver, O. and Leung, J.W.T. (2018). Biomarkers and imaging of breast cancer. *Am. J. Roentgenol.* 210 (2): 271–278.

12 Misek, D.E. and Kim, E.H. (2011). Protein biomarkers for the early detection of breast cancer. *Int. J. Proteomics* 2011: 343582. https://doi .org/10.1155/2011/343582.

13 Harbeck, N. and Gnant, M. (2017). Breast cancer. *Lancet* 389: 1134–1150.

14 Li, G., Hu, J., and Hu, G. (2017). Biomarker studies in early detection and prognosis of breast cancer. *Adv. Exp. Med. Biol.* 1026: 27–39.

15 Jayanthi, V., Das, A.B., and Saxena, U. (2017). Recent advances in biosensor development for the detection of cancer biomarkers. *Biosens. Bioelectron.* 91: 15–23.

16 Tothill, I.E. (2009). Biosensors for cancer markers diagnosis. *Semin. Cell Dev. Biol.* 20: 55–62.

17 Chang, Y., Xu, J., and Zhang, Q. (2017). Microplate magnetic chemiluminescence immunoassay for detecting urinary survivin in bladder cancer. *Oncol. Lett.* 14: 4043–4052.

18 Lakshmipriya, T., Gopinath, S.C.B., Hashim, U., and Murugaiyah, V. (2017). Multi-analyte validation in heterogeneous solution by ELISA. *Int. J. Biol. Macromol.* 105: 796–800.

19 Yang, G., Xiao, Z., Tang, C. et al. (2019). Recent advances in biosensor for detection of lung cancer biomarkers. *Biosens. Bioelectron.* 141: 111416. https://doi .org/10.1016/j.bios.2019.111416.

20 He, Z., Chen, Z., Tan, M. et al. (2020). A review on methods for diagnosis of breast cancer cells and tissues. *Cell Proliferation* 53: e12822. https://doi.org/10.1111/ cpr.12822.

21 Ayer, T. (2015). Inverse optimization for assessing emerging technologies in breast cancer screening. *Ann. Oper. Res.* 230 (1): 57–85.

22 Nelson, H.D., Tyne, K., Naik, A. et al., U.S. Preventive Services Task Force(2009). Screening for breast cancer: an update for the U.S. Preventive Services Task Force. *Ann. Intern. Med.* 151: 727–737.

23 Pisano, E.D., Gatsonis, C., Hendrick, E. et al. (2005). Diagnostic performance of digital versus film mammography for breast-cancer screening. *N. Engl. J. Med.* 353: 1773–1783.

24 Covington, M.F., Pizzitola, V.J., Lorans, R. et al. (2018). The future of contrast-enhanced mammography. *Am. J. Roentgenol.* 210 (2): 292–300.

25 Chong, A., Weinstein, S.P., McDonald, E.S., and Conant, E.F. (2019). Digital breast tomosynthesis: concepts and clinical practice. *Radiology* 292 (1): 1–14.

26 Fallenberg, E.M., Schmitzberger, F.F., Amer, H. et al. (2017). Contrast enhanced spectral mammography vs. mammography and MRI – clinical performance in a multi-reader evaluation. *Eur. Radiol.* 27 (7): 2752–2764.

27 Sorin, V., Yagil, Y., Yosepovich, A. et al. (2018). Contrast-enhanced spectral mammography in women with intermediate breast cancer risk and dense breasts. *Am. J. Roentgenol.* 211 (5): 267–274.

28 Lu, Z., Hao, C., Pan, Y. et al. (2020). Contrast-Enhanced Spectral Mammography Versus Ultrasonography: Diagnostic Performance in Symptomatic Patients with Dense Breasts. *Korean J. Radiol.* 21 (4): 442–449. https://doi.org/10.3348/kjr.2019.0393.

29 Skaane, P., Sebuodegard, S., Bandos, A.I. et al. (2018). Performance of breast cancer screening using digital breast tomosynthesis: results from the prospective population-based Oslo Tomosynthesis Screening Trial. *Breast Cancer Res. Treat.* 169 (3): 489–496.

30 Katzen, J. and Dodelzon, K. (2018). A review of computer aided detection in mammography. *Clin Imaging.* 52: 305–309.

31 Danala, G., Patel, B., Aghaei, F. et al. (2018). Classification of breast masses using a computer-aided diagnosis scheme of contrast enhanced digital mammograms. *Ann. Biomed. Eng.* 46 (9): 1419–1431.

32 Benedikt, R.A., Boatsman, J.E., Swann, C.A. et al. (2018). Concurrent computer-aided detection improves reading time of digital breast tomosynthesis and maintains interpretation performance in a multireader multicase study. *Am. J. Roentgenol.* 210 (3): 685–694.

33 Andersson, I., Ikeda, D.M., Zackrisson, S. et al. (2008). Breast tomosynthesis and digital mammography: a comparison of breast cancer visibility and BIRADS classification in a population of cancers with subtle mammographic findings. *Eur. Radiol. 18*: 2817–2825. (copyright taken, License no.- 5493691267918).

34 Khamparia, A., Bharati, S., Podder, P. et al. (2021). Diagnosis of breast cancer based on modern mammography using hybrid transfer learning. *Multidimension. Syst. Signal Process.* 32: 747–765. https://doi.org/10.1007/s11045-02000756-713.

35 Montaha, S., Azam, S., Rafid, A.K.M.R.H. et al. (2021). BreastNet18: a high accuracy fine-tuned VGG16 model evaluated using ablation study for diagnosing breast cancer from enhanced mammography images. *Biology* 10: 1347.

36 Monticciolo, D.L., Newell, M.S., Hendrick, R.E. et al. (2017). Breast cancer screening for average-risk women: recommendations from the ACR commission on breast imaging. *J. Am. Coll. Radiol.* 14 (9): 1137–1143.

37 Ha, R., Kim, H., Mango, V. et al. (2014). Ultrasonographic features and clinical implications of benign palpable breast lesions in young women. *Ultrasonography* 34 (1): 66–70.

38 Zhang, H., Shi, Q., Gu, J. et al. (2014). Combined value of virtual touch tissue quantification and conventional sonographic features for differentiating benign and malignant thyroid nodules smaller than 10 mm. *J. Ultrasound Med.* 33 (2): 257–264.

39 Dhabyani, W.A., Gomaa, M., Khaled, H., and Fahmy, A. (2020). Dataset of breast ultrasound images. *Data Brief* 28: 104863. https://doi.org/10.1016/j.dib.2019.104863.

40 Helal, M.H., Mansour, S.M., Salaleldin, L.A. et al. (2018). The impact of contrast-enhanced spectral mammogram (CESM) and three-dimensional breast ultrasound (3DUS) on the characterization of the disease extend in cancer patients. *Br. J. Radiol.* 91 (1087): 20170977.

41 Yang, G.C.H. and Fried, K.O. (2017). Most thyroid cancers detected by sonography lack intranodular vascularity on color doppler imaging: review of the literature and sonographic-pathologic correlations for 698 thyroid neoplasms. *J. Ultrasound Med.* 36 (1): 89–94.

42 Krouskop, T.A., Wheeler, T.M., Kallel, F. et al. (1998). Elastic moduli of breast and prostate tissues under compression. *Ultrason Imaging* 20 (4): 260–274.

43 Adimule, V., Yallur, B.C., Pai, M.M. et al. (2022). Biogenic synthesis of magnetic palladium nanoparticles decorated over reduced graphene oxide using *Piper betle* Petiole extract (Pd-rGO@Fe_3O_4 NPs) as heterogeneous hybrid nanocatalyst for applications in Suzuki–Miyaura coupling reactions of biphenyl compounds. *Top. Catal.* https://doi.org/10.1007/s11244-022-01672-9.

44 Signore, G., Nifosì, R., Albertazzi, L. et al. (2010). Polarity sensitive coumarins tailored to live cell imaging. *J. Am. Chem. Soc.* 132 (4): 1276–1288.

45 Mohan Gift, M.D., Pattnaik, B., Nandi, S.S. et al. (2022). Determination of prohibition mechanism of cationic polymer/SiO_2 composite as inhibitor in water using drilling fluid. *Mater. Today Proc.* https://doi.org/10.1016/j .matpr.2022.08.171.

46 Park, A.Y., Seo, B.K., Cha, S.H. et al. (2016). An innovative ultrasound technique for evaluation of tumor vascularity in breast cancers: superb micro-vascular imaging. *J. Breast Cancer* 19 (2): 210.

47 Machado, P., Eisenbrey, J.R., Stanczak, M. et al. (2019). Characterization of breast microcalcifications using a new ultrasound image-processing technique. *J. Ultrasound Med.* 38 (7): 1733–1738.

48 Machado, P., Eisenbrey, J.R., Stanczak, M. et al. (2018). Ultrasound detection of microcalcifications in surgical breast specimens. *Ultrasound Med Biol.* 44 (6): 1286–1290.

49 Hooley, R.J., Scoutt, L.M., and Philpotts, L.E. (2013). Breast ultrasonography: State of the art. *Radiology.* 268: 642–659.

50 Shen, Y., Shamout, F.E., Oliver, J.R. et al. (2021). Artificial intelligence system reduces false-positive findings in the interpretation of breast ultrasound exams. *Nat. Commun.* 12: 5645. https://doi.org/10.1038/s41467-021-26023-2.

51 Riedl, C.C., Luft, N., Bernhart, C. et al. (2015). Triple-modality screening trial for familial breast cancer underlines the importance of magnetic resonance imaging and questions the role of mammography and ultrasound regardless of patient mutation status, age, and breast density. *J. Clin. Oncol.* 33 (10): 1128–1135.

52 Kuhl, C. (2007). The current status of breast MR imaging. Part I. Choice of technique, image interpretation, diagnostic accuracy, and transfer to clinical practice. *Radiology* 244: 356–378.

53 Mann, R.M., Kuhl, C.K., and Moy, L. (2019). Contrast-enhanced MRI for breast cancer screening. *J. Magn. Reson. Imaging.* 50: 377–390.

54 Moy, L., Noz, M.E., Maguire, G.Q. Jr. et al. (2010). Role of fusion of prone FDGPET and magnetic resonance imaging of the breasts in the evaluation of breast cancer. *Breast J.* 16 (4): 369–376.

55 Onishi, N., Sadinski, M., Hughes, M.C. et al. (2020). Ultrafast dynamic contrast-enhanced breast MRI may generate prognostic imaging markers of breast cancer. *Breast Cancer Res.* 22: 58.

56 Orguc, S., Basara, I., and Coskun, T. (2012). Diffusion-weighted MR imaging of the breast: comparison of apparent diffusion coefficient values of normal breast tissue with benign and malignant breast lesions. *Singapore Med. J.* 53 (11): 737–743.

57 Bougias, H., Ghiatas, A., Priovolos, D. et al. (2016). Whole-lesion apparent diffusion coefficient (ADC) metrics as a marker of breast tumour characterization – comparison between ADC value and ADC entropy. *Br. J. Radiol.* 89 (1068): 20160304.

58 Rahbar, H. and Partridge, S.C. (2016). Multiparametric MR imaging of breast cancer. *Magn. Reson. Imaging Clin. N. Am.* 24: 223–238.

59 Yabuuchi, H., Matsuo, Y., Sunami, S. et al. (2011). Detection of non-palpable breast cancer in asymptomatic women by using unenhanced diffusion-weighted and T2-weighted MR imaging: comparison with mammography and dynamic contrast-enhanced MR imaging. *Eur. Radiol.* 21: 11–17.

60 Sharma, U. and Jagannathan, N.R. (2022). Magnetic resonance imaging (MRI) and MR spectroscopic methods in understanding breast cancer biology and metabolism. *Metabolites* 12: 295. https://doi.org/10.3390/metabo12040295.

61 Clauser, P., Marcon, M., Dietzel, M. et al. (2017). A new method to reduce false positive results in breast MRI by evaluation of multiple spectral regions in proton MR-spectroscopy. *Eur. J. Radiol.* 92: 51–57.

62 He, D., Mustafi, D., Fan, X. et al. (2018). Magnetic resonance spectroscopy detects differential lipid composition in mammary glands on low fat, high animal fat versus high fructose diets. *PLoS One* 13 (1): e0190929.

63 Cheng, L.L., Chang, I.W., Smith, B.L., and Gonzalez, R.G. (1998). Evaluating human breast ductal carcinomas with high-resolution magic-angle spinning proton magnetic resonance spectroscopy. *J. Magn. Reson.* 135: 194–202.

64 Sitter, B., Lundgren, S., Bathen, T.F. et al. (2006). Comparison of HR-MAS MR spectroscopic profiles of breast cancer tissue with clinical parameters. *NMR Biomed.* 19: 30–40.

65 Sitter, B., Sonnewald, U., Spraul, M. et al. (2002). High-resolution magic angle spinning MRS of breast cancer tissue. *NMR Biomed.* 15: 327–337.

66 Choi, J., Baek, H.M., Kim, S. et al. (2012). HR-MAS MR spectroscopy of breast cancer tissue obtained with core needle biopsy: correlation with prognostic factors. *PLoS One* 7: e51712.

67 Maria, R.M., Altei, W.F., Selistre-de-Araujo, H.S., and Colnago, L.A. (2017). Impact of chemotherapy on metabolic reprogramming: characterization of the metabolic profile of breast cancer MDA-MB-231 cells using ^{1}H HR-MAS NMR spectroscopy. *J. Pharm. Biomed. Anal.* 146: 324–328.

68 Fuss, T.L. and Cheng, L.L. (2016). Evaluation of cancer metabolomics using ex vivo high resolution magic angle spinning (HRMAS) magnetic resonance spectroscopy (MRS). *Metabolites* 6: 11.

69 Jagannathan, N.R., Kumar, M., Seenu, V. et al. (2001). Evaluation of total choline from in vivo volume localized proton MR spectroscopy and its response to neoadjuvant chemotherapy in locally advanced breast cancer. *Br. J. Cancer* 84: 1016–1022.

70 Sah, R.G., Sharma, U., Parshad, R. et al. (2012). Association of estrogen receptor, progesterone receptor, and human epidermal growth factor receptor 2 status with total choline concentration and tumor volume in breast cancer patients: an MRI and in vivo proton MRS study. *Magn. Reson. Med.* 68: 1039–1047.

71 Katz-Brull, R., Lavin, P.T., and Lenkinski, R.E. (2002). Clinical utility of proton magnetic resonance spectroscopy in characterizing breast lesions. *J. Natl. Cancer Inst.* 94: 1197–1203.

72 Keri, R.S., Adimule, V., Kendrekar, P. et al. (2022). The nano-based catalyst for the synthesis of benzimidazoles. *Top. Catal.* 64: 1–21.

73 Baltzer, P.A. and Dietzel, M. (2013). Breast lesions: diagnosis by using proton MR spectroscopy at 1.5 and 3.0 T – systematic review and meta-analysis. *Radiology* 267: 735–746.

74 Adimule, V., Nandi, S.S., Yallur, B.C., and Shaikh, N. (2021). CNT/graphene-assisted flexible thin-film preparation for stretchable electronics and superconductors. In: *Sensors for Stretchable Electronics in Nanotechnology* (ed. K. Pal), 89–103. CRC Press.

75 Wang, X., Wang, X.J., Song, H.S., and Chen, L.H. (2015). ^{1}H-MRS evaluation of breast lesions by using total choline signal-to-noise ratio as an indicator of malignancy: a meta-analysis. *Med. Oncol.* 32: 160.

76 Adimule, V., Yallur, B.C., Batakurki, S., and Nandi, S.S. (2022). Synthesis, morphology and enhanced optical properties of novel $Gd_xCo_3O_4$ nanostructures. *Adv. Mater. Res.* 1173: 71–82. Trans Tech Publications, Ltd.

77 Gallagher, F.A., Woitek, R., McLean, M.A. et al. (2020). Imaging breast cancer using hyperpolarized carbon-13 MRI. *Proc. Natl. Acad. Sci. U.S.A.* 117: 2092–2098.

78 Bohte, A.E., Nelissen, J.L., Runge, J.H. et al. (2018). Breast magnetic resonance elastography: a review of clinical work and future perspectives. *NMR Biomed.* 31 (10): e3932.

79 Adimule, V., Medapa, S., Rao, P.K., and Kumar, L.S. (2014). Synthesis of Schiff bases of 5-[5-(4-fluorophenyl)thiophen-2-yl]-1,3,4-thiadiazol-2-amine and its anticancer activity. *Int. J. Adv. Pharm. Sci.* 5 (1): 1761–1768.

80 Albano, D., Bosio, G., Orlando, E. et al. (2017). Role of fluorine-18-fluorodeoxyglucose positron emission tomography/computed tomography in evaluating breast mucosa-associated lymphoid tissue lymphoma: a case series. *Hematol. Oncol.* 35 (4): 884–889.

81 Romeo, V., Clauser, P., Rasul, S. et al. (2022). AI-enhanced simultaneous multiparametric ^{18}F-FDG PET/MRI for accurate breast cancer diagnosis. *Eur. J. Nucl. Med. Mol. Imaging* 49: 596–608.

82 Tagliafico, A.S., Piana, M., Schenone, D. et al. (2020). Overview of radiomics in breast cancer diagnosis and prognostication. *Breast* 49: 74–80.

83 Adimule, V., Yallur, B., and Gowda, A. (2022). Crystal structure, morphology, optical and super-capacitor properties of Sr_x: **α**-Sb_2O_4 nanostructures. *Anal. Bioanal. Electrochem.* 14 (1): 1–17.

84 Crivelli, P., Ledda, R.E., Parascandolo, N. et al. (2018). A new challenge for radiologists: radiomics in breast cancer. *BioMed. Res. Int.* 2018: 6120703.

85 AlSawaftah, N., El-Abed, S., Dhou, S., and Zakaria, A. (2022). Microwave imaging for early breast cancer detection: current state, challenges, and future directions. *J. Imaging* 8: 123. https://doi.org/10.3390/jimaging8050123.

86 Batakurki, S.R., Adimule, V., Pai, M.M. et al. (2022). Synthesis of Cs-Ag/Fe_2O_3 nanoparticles using *Vitis labrusca* Rachis extract as green hybrid nanocatalyst for the reduction of arylnitro compounds. *Top. Catal.* https://doi.org/10.1007/s11244-022-01593-7.

87 Hamidipour, A., Henriksson, T., Hopfer, M. et al. (2018). Electromagnetic tomography for brain imaging and stroke diagnostics: progress towards clinical application. In: *Emerging Electromagnetic Technologies for Brain Diseases Diagnostics, Monitoring and Therapy* (ed. L. Crocco, I. Karanasiou, M.L. James, and R.C. Conceição), 59–86. Springer.

88 Semenov, S., Kellam, J., Sizov, Y. et al. (2011). Microwave tomography of extremities: 1. Dedicated 2D system and physiological signatures. *Phys. Med. Biol.* 56: 2005.

89 Meaney, P.M., Goodwin, D., Golnabi, A.H. et al. (2012). Clinical microwave tomographic imaging of the calcaneus: a first-in-human case study of two subjects. *IEEE Trans. Biomed. Eng.* 59: 3304–3313.

90 Zamani, A., Rezaeieh, S.A., Bialkowski, K.S., and Abbosh, A.M. (2017). Boundary estimation of imaged object in microwave medical imaging using antenna resonant frequency shift. *IEEE Trans. Antennas Propag.* 66: 927–936.

91 Adimule, V., Bhat, V.S., Yallur, B.C. et al. (2022). Facile synthesis of novel $SrO_{0.5}$:$MnO_{0.5}$ bimetallic oxide nanostructure as a high-performance electrode material for supercapacitors. *Nanomater. Nanotechnol.* 12: 1–14. https://doi.org/10.1177/18479804211064028.

92 Grzegorczyk, T.M., Meaney, P.M., Kaufman, P.A., and Paulsen, K.D. (2012). Fast 3-D tomographic microwave imaging for breast cancer detection. *IEEE Trans. Med. Imaging* 31: 1584–1592.

93 Modiri, A., Goudreau, S., Rahimi, A., and Kiasaleh, K. (2017). Review of breast screening: toward clinical realization of microwave imaging. *Med. Phys.* 44: e446–e458.

94 Campbell, A. and Land, D. (1992). Dielectric properties of female human breast tissue measured in vitro at 3.2 GHz. *Phys. Med. Biol.* 37: 193.

95 Shaikh, N.M., Bagihalli, G.B., Adimule, V. et al. (2022). A novel silica immobilized acidic ionic liquid [BMIM][$AlCl_4$] as an effective catalyst for biscoumarine synthesis. *Top. Catal.* https://doi.org/10.1007/s11244-022-01591-9.

96 Meaney, P.M., Fanning, M.W., di Florio-Alexander, R.M. et al. (2010). Microwave tomography in the context of complex breast cancer imaging. In: *Proceedings of the 2010 Annual International Conference of the IEEE Engineering in Medicine and*

Biology Society (EMBC), Buenos Aires, Argentina (31 August–4 September 2010), 3398–3401. http://doi.org/10.1109/IEMBS.2010.5627932.

97 Adimule, V., Nandi, S.S., and Yallur, B.C. (2022). Devices and sensors based on additively manufactured shape-memory of hybrid nanocomposites. In: *Shape Memory Composites Based on Polymers and Metals for 4D Printing* (ed. M.R. Maurya, K.K. Sadasivuni, J.J. Cabibihan, et al.), 341–359. Cham: Springer. https://doi.org/10.1007/978-3-030-94114-7_15.

98 Li, D., Meaney, P.M., Raynolds, T. et al. (2004). Parallel-detection microwave spectroscopy system for breast imaging. *Rev. Sci. Instrum.* 75: 2305–2313.

99 Meaney, P.M., Paulsen, K.D., Hartov, A., and Crane, R.K. (1995). An active microwave imaging system for reconstruction of 2-D electrical property distributions. *IEEE Trans. Biomed. Eng.* 42: 1017–1026.

100 Bulyshev, A.E., Semenov, S.Y., Souvorov, A.E. et al. (2001). Computational modeling of three-dimensional microwave tomography of breast cancer. *IEEE Trans. Biomed. Eng.* 48: 1053–1056.

101 Meaney, P.M., Fanning, M.W., Li, D. et al. (2000). A clinical prototype for active microwave imaging of the breast. *IEEE Trans. Microwave Theory Tech.* 48: 1841–1853.

102 Meaney, P.M., Fanning, M.W., Raynolds, T. et al. (2007). Initial clinical experience with microwave breast imaging in women with normal mammography. *Acad. Radiol.* 14: 207–218.

103 Adimule, V., Yallur, B.C., and Gowda, A.H.J. (2022). Advanced sensors based on carbon nanomaterials. In: *Carbon Nanomaterials-Based Sensors* (ed. J.G. Manjunatha and C.M. Hussain), 259–268. Elsevier. https://doi.org/10.1016/B978-0-323-91174-0.00004-4.

104 Zhu, X., Zhao, Z., Wang, J. et al. (2013). Microwave-induced thermal acoustic tomography for breast tumor based on compressive sensing. *IEEE Trans. Biomed. Eng.* 60: 1298–1307.

105 Bevacqua, M.T. and Scapaticci, R. (2016). A compressive sensing approach for 3D breast cancer microwave imaging with magnetic nanoparticles as contrast agent. *IEEE Trans. Med. Imaging* 35: 665–673.

106 Bridges, J.E. (1998). Non-invasive system for breast cancer detection. US Patent 5704355A.

107 Nandi, S.S., Suryavanshi, A., Adimule, V., and Yallur, B.C. (2020). Super capacitor characteristics of novel rare earth perovskite nanomaterials of $Sr_{0.5}$, $Cu_{0.4}$, $Y_{0.1}$. *AIP Conf. Proc.* 2274: 020007. https://doi.org/10.1063/5.0022454.

108 Fear, E.C. (2005). Microwave imaging of the breast. *Technol. Cancer Res. Treat.* 4: 69–82.

109 Bidhendi, H.K., Jafari, H.M., and Genov, R. (2014). Ultra-wideband imaging systems for breast cancer detection. In: *Ultra-Wideband and 60 GHz Communications for Biomedical Applications* (ed. M.R. Yuce), 83–103. Boston, MA: Springer.

110 Hagness, S.C., Taflove, A., and Bridges, J.E. (1998). Two-dimensional FDTD analysis of a pulsed microwave confocal system for breast cancer detection: fixed-focus and antenna-array sensors. *IEEE Trans. Biomed. Eng.* 45: 1470–1479.

111 Hagness, S.C., Taflove, A., and Bridges, J.E. (1999). Three-dimensional FDTD analysis of a pulsed microwave confocal system for breast cancer detection: Design of an antenna-array element. *IEEE Trans. Antennas Propag.* 47: 783–791.

112 Klemm, M., Craddock, I., Leendertz, J. et al. (2008). Experimental and clinical results of breast cancer detection using UWB microwave radar. In: *Proceedings of the 2008 IEEE Antennas and Propagation Society International Symposium*, San Diego, CA, USA (5–12 July 2008), 1–4. IEEE.

113 Klemm, M., Craddock, I.J., Leendertz, J.A. et al. (2009). Radar-based breast cancer detection using a hemispherical antenna array – experimental results. *IEEE Trans. Antennas Propag.* 57: 1692–1704.

114 Henriksson, T., Klemm, M., Gibbins, D. et al. (2011). Clinical trials of a multistatic UWB radar for breast imaging. In: *Proceedings of the 2011 Loughborough Antennas & Propagation Conference*, Loughborough, UK (14–15 November 2011) (ed. Z. Shen), 1–4. IEEE.

115 Fear, E. and Sill, J. (2003). Preliminary investigations of tissue sensing adaptive radar for breast tumor detection. In: *Proceedings of the 25th Annual International Conference of the IEEE Engineering in Medicine and Biology Society*, Cancun, Mexico (17–21 September 2003), vol. 4, 3787–3790. IEEE (IEEE Cat. No. 03CH37439).

116 Williams, T.C., Fear, E.C., and Westwick, D.T. (2006). Tissue sensing adaptive radar for breast cancer detection – investigations of an improved skin-sensing method. *IEEE Trans. Microwave Theory Tech.* 54: 1308–1314.

117 Adimule, V., Suryavanshi, A., and Nandi, S. (2020). Synthesis, characterization and impedance studies of novel nanocomposites of gadolinium titanate. *IOP Conf. Ser.: Mater. Sci. Eng.* 872: 012099. https://iopscience.iop.org/article/10.1088/1757-899X/872/1/012099/meta.

118 Guang-dong, L. and Ye-rong, Z. (2010). An overview of active microwave imaging for early breast cancer detection. *J. Nanjing Univ. Posts Telecommun.* 30: 64–70.

119 Bond, E.J., Li, X., Hagness, S.C., and Van Veen, B.D. (2003). Microwave imaging via space-time beamforming for early detection of breast cancer. *IEEE Trans. Antennas Propag.* 51: 1690–1705.

120 Elsdon, M., Leach, M., Skobelev, S., and Smith, D. (2007). Microwave holographic imaging of breast cancer. In: *Proceedings of the 2007 International Symposium on Microwave, Antenna, Propagation and EMC Technologies for Wireless Communications*. Hangzhou, China (16–17 August 2007) (ed. G.E. Ponchak), 966–969. IEEE.

121 Adimule, V., Vageesha, P., Bagihalli, G. et al. (2019). Synthesis, characterization of hybrid nanomaterials of strontium, yttrium, copper doped with indole Schiff base derivatives possessing dielectric and semiconductor properties. In: *Emerging Research in Electronics, Computer Science and Technology*, Lecture Notes in Electrical Engineering, vol. 545 (ed. V. Sridhar, M. Padma, and K. Rao). Singapore: Springer. https://doi.org/10.1007/978-981-13-5802-9_97.

122 Wang, L., Simpkin, R., and Al-Jumaily, A. (2013). Holographic microwave imaging array: experimental investigation of breast tumour detection. In: *Proceedings of the 2013 IEEE International Workshop on Electromagnetics, Applications and Student*

Innovation Competition, Hong Kong, China (1–3 August 2013) (ed. K.K. So and C.K. Leung), 61–64. IEEE.

123 Wang, L. and Fatemi, M. (2018). Compressive sensing holographic microwave random array imaging of dielectric inclusion. *IEEE Access* 6: 56477–56487.

124 Adimule, V., Yallur, B.C., Challa, M., and Joshi, R.S. (2021). Synthesis of hierarchical structured Gd doped **α**-Sb_2O_4 as an advanced nanomaterial for high performance energy storage devices. *Heliyon* 7 (12): e08541. https://doi.org/10.1016/j.heliyon.2021.e08541.

125 Zhang, T., Hu, H., Yan, G. et al. (2019). Long non-coding RNA and breast cancer. *Technol. Cancer Res. Treat.* 18: 1533033819843889.

126 Wang, H., Peng, R., Wang, J. et al. (2018). Circulating microRNAs as potential cancer biomarkers: the advantage and disadvantage. *Clin. Epigenet.* 10: 59.

127 Liang, D., Liu, H., Yang, Q. et al. (2020). Long noncoding RNA RHPN1-AS1, induced by KDM5B, is involved in breast cancer via sponging miR-6884-5p. *J. Cell. Biochem.* https://doi.org/10.1002/jcb.29645.

128 Jahani, S., Nazeri, E., Majidzadeh, A.K. et al. (2020). Circular RNA; a new biomarker for breast cancer: a systematic review. *J. Cell. Physiol.* 235: 5501–5510.

129 Zhao, Q., Yang, Y., Ren, G. et al. (2019). Integrating bipartite network projection and KATZ measure to identify novel circRNA-disease associations. *IEEE Trans. Nanobiosci.* 18: 578–584.

130 Ye, Z., Wang, C., Wan, S. et al. (2019). Association of clinical outcomes in metastatic breast cancer patients with circulating tumour cell and circulating cell-free DNA. *Eur. J. Cancer* 106: 133–143.

131 Openshaw, M.R., Page, K., Fernandez-Garcia, D. et al. (2016). The role of ctDNA detection and the potential of the liquid biopsy for breast cancer monitoring. *Expert Rev. Mol. Diagn.* 16: 751–755.

132 Tellez-Gabriel, M., Knutsen, E., and Perander, M. (2020). Current status of circulating tumor cells, circulating tumor DNA, and exosomes in breast cancer liquid biopsies. *Int. J. Mol. Sci.* 21: 9457.

133 Adimule, V., Bowmik, D., and Adarsha, H.J. (2020). A facile synthesis of Cr doped WO_3 nanocomposites and its effect in enhanced current–voltage and impedance characteristics of thin films. *Lett. Mater.* 10 (4): 481–485.

134 Barkal, A.A., Brewer, R.E., Markovic, M. et al. CD24 signalling through macrophage Siglec-10 is a target for cancer immunotherapy. *Nature* 572: 392–396.

135 Wang, Z., Wang, Q., Wang, Q. et al. (2017). Prognostic significance of CD24 and CD44 in breast cancer: a meta-analysis. *Int. J. Biol. Markers* 32: e75–e82.

136 Adimule, V., Nandi, S.S., and Jagadeesha Gowda, A.H. (2021). Enhanced power conversion efficiency of the P3BT (poly-3-butyl thiophene) doped nanocomposites of Gd-TiO_3 as working electrode. In: *Techno-Societal 2020* (ed. P.M. Pawar, R. Balasubramaniam, B.P. Ronge, et al.). Cham: Springer. https://doi.org/10.1007/978-3-030-69925-3_6.

137 Senbanjo, L.T. and Chellaiah, M.A. (2017). CD44: a multifunctional cell surface adhesion receptor is a regulator of progression and metastasis of cancer cells. *Front. Cell Dev. Biol.* 5: 18.

138 Adimule, V., Suryavanshi, A., Yallur, B.C., and Nandi, S.S. (2020). A facile synthesis of poly(3-octyl thiophene):$Ni_{0.4}Sr_{0.6}TiO_3$ hybrid nanocomposites for solar cell applications. *Macromol. Symp.* 392: 2000001.

139 Zhou, R., Yazdanifar, M., Roy, L.D. et al. (2019). CAR T-cells targeting the tumor MUC1 glycoprotein reduce triple-negative breast cancer growth. *Front. Immunol.* 10: –1149.

140 Diaconu, I., Cristea, C., Harceaga, V. et al. (2013). Electrochemical immunosensors in breast and ovarian cancer. *Clin. Chim. Acta* 425: 128–138.

141 Hong, R., Sun, H., Li, D. et al. (2022). A review of biosensors for detecting tumor markers in breast cancer. *Life* 12: 342. https://doi.org/10.3390/life12030342.

142 Cristofanilli, M., Pierga, J.Y., Reuben, J. et al. (2019). The clinical use of circulating tumor cells (CTCs) enumeration for staging of metastatic breast cancer (MBC): international expert consensus paper. *Crit. Rev. Oncol. Hematol.* 134: 39–45.

143 Adimule, V., Yallur, B.C., and Sharma, K. (2022). Studies on crystal structure, morphology, optical and photoluminescence properties of flake-like Sb doped Y_2O_3 nanostructures. *J. Opt.* 51: 173–183. https://doi.org/10.1007/s12596-021-00746-3.

144 Zhou, Y.U., Xu, H., Wang, H. et al. (2020). Detection of breast cancer-derived exosomes using the horseradish peroxidase-mimicking DNAzyme as an aptasensor. *Analyst* 145 (1): 107–114.

145 Nicolini, A., Ferrari, P., and Duffy, M.J. (2018). Prognostic and predictive biomarkers in breast cancer: past, present and future. *Semin. Cancer Biol.* 52: 56–73.

146 Suryavanshi, A., Adimule, V., and Nandi, S.S. (2020). Synthesis, impedance, and current–voltage characteristics of strontium-manganese titanate hybrid nanoparticles. *Macromol. Symp.* 392: 2000002.

147 Adimule, V., Yallur, B.C., Bhowmik, D. et al. (2021). Morphology, structural and photoluminescence properties of shaping triple semiconductor $Y_xCoO:ZrO_2$ nanostructures. *J. Mater. Sci. – Mater. Electron.* 32: 12164–12181. https://doi.org/10.1007/s10854-021-05845-2.

148 Roointan, A., Ahmad, M.T., Ibrahim, W.S. et al. (2019). Early detection of lung cancer biomarkers through biosensor technology: a review. *J. Pharm. Biomed. Anal.* 164: 93–103.

149 Ranjan, P., Parihar, A., Jain, S. et al. (2020). Biosensor-based diagnostic approaches for various cellular biomarkers of breast cancer: a comprehensive review. *Anal. Biochem.* 610: 113996.

150 Kal-Koshvandi, A.T. (2020). Recent advances in optical biosensors for the detection of cancer biomarker **α**-fetoprotein (AFP). *TrAC, Trends Anal. Chem.* 128: 115920.

151 Piroozmand, F., Mohammadipanah, F., and Faridbod, F. (2020). Emerging biosensors in detection of natural products. *Synth. Syst. Biotechnol.* 5: 293–303.

152 Adimule, V., Revaigh, M.G., and Adarsha, H.J. (2020). Synthesis and fabrication of Y-doped ZnO nanoparticles and their application as a gas sensor for the detection of ammonia. *J. Mater. Eng. Perform.* 29: 4586–4596. https://doi.org/10.1007/s11665-020-04979-4.

153 Ouyang, M., Tu, D., Tong, L. et al. (2021). A review of biosensor technologies for blood biomarkers toward monitoring cardiovascular diseases at the point-of-care. *Biosens. Bioelectron.* 171: 112621.

154 Xu, L., Shoaie, N., Jahanpeyma, F. et al. (2020). Optical, electrochemical and electrical (nano)biosensors for detection of exosomes: a comprehensive overview. *Biosens. Bioelectron.* 161: 112222.

155 Sadighbayan, D., Sadighbayan, K., Khosroushahi, A.Y., and Hasanzadeh, M. (2019). Recent advances on the DNA-based electrochemical biosensing of cancer biomarkers: analytical approach. *TrAC, Trends Anal. Chem.* 119: 115609.

156 Sharifi, M., Avadi, M.R., Attar, F. et al. (2019). Cancer diagnosis using nanomaterials based electrochemical nanobiosensors. *Biosens. Bioelectron.* 126: 773–784.

157 Adimule, V., Kerur, S.S., Chinnam, S. et al. (2022). Guar gum and its nanocomposites as prospective materials for miscellaneous applications: a short review. *Top. Catal.* https://doi.org/10.1007/s11244-022-01587-5.

158 Nandi, S.S., Suryavanshi, A., Adimule, V., and Maradur, S.R. (2020). Semiconductor current–voltage characteristics of some novel perovskite ionic nanocomposites of $Sr_{0.5}$, $Cu_{0.4}$, $Y_{0.1}$ and $Sr_{0.5}$, $Mn_{0.5}$ and their electronic sensor applications. *AIP Conf. Proc.* 2274: 020006: https://doi.org/10.1063/5.0022453.

159 Mittal, S., Kaur, H., Gautam, N., and Mantha, A.K. (2017). Biosensors for breast cancer diagnosis: a review of bioreceptors, biotransducers and signal amplification strategies. *Biosens. Bioelectron.* 88: 217–231.

160 Arya, S.K., Wang, K.Y., Wong, C.C., and Rahman, A.R. (2013). Anti-EpCAM modified LC-SPDP monolayer on gold microelectrode based electrochemical biosensor for MCF-7 cells detection. *Biosens. Bioelectron.* 41: 446.

161 Hong, C., Yuan, R., Chai, Y., and Zhuo, Y. (2019). Ferrocenyl-doped silica nanoparticles as an immobilized affinity support for electrochemical immunoassay of cancer antigen 15-3. *Anal. Chim. Acta* 633: 244–249.

162 Vasudev, A., Kaushik, A., and Bhansali, S. (2013). Electrochemical immunosensor for label free epidermal growth factor receptor (EGFR) detection. *Biosens. Bioelectron.* 39: 300–305.

163 Hakimian, F. and Ghourchian, H. (2020). Ultrasensitive electrochemical biosensor for detection of microRNA-155 as a breast cancer risk factor. *Anal. Chim. Acta* 1136: 1–8.

164 Wang, J., Wang, D., and Hui, N. (2020). A low fouling electrochemical biosensor based on the zwitterionic polypeptide doped conducting polymer PEDOT for breast cancer marker BRCA1 detection. *Bioelectrochemistry* 136: 107595.

165 Han, R., Wang, G., Xu, Z. et al. (2020). Designed antifouling peptides planted in conducting polymers through controlled partial doping for electrochemical detection of biomarkers in human serum. *Biosens. Bioelectron.* 164: 112317.

166 Xia, Y.M., Li, M.Y., Chen, C.L. et al. (2020). Employing label-free electrochemical biosensor based on 3D-reduced graphene oxide and polyaniline nanofibers for ultrasensitive detection of breast cancer BRCA1 biomarker. *Electroanalysis* 32: 2045–2055.

167 Chang, J., Wang, X., Wang, J. et al. (2019). Nucleic acid-functionalized metal-organic framework-based homogeneous electrochemical biosensor for simultaneous detection of multiple tumor biomarkers. *Anal. Chem.* 91: 3604–3610.

168 Wang, H., Sun, J., Lu, L. et al. (2020). Competitive electrochemical aptasensor based on a cDNA ferrocene/MXene probe for detection of breast cancer marker Mucin1. *Anal. Chim. Acta* 1094: 18–25.

169 Xu, S., Chang, Y., Wu, Z. et al. (2020). One DNA circle capture probe with multiple target recognition domains for simultaneous electrochemical detection of miRNA-21 and miRNA-155. *Biosens. Bioelectron.* 149: 111848.

170 Marques, R.C., Viswanathan, S., Nouws, H.P. et al. (2014). Electrochemical immunosensor for the analysis of the breast cancer biomarker HER2 ECD. *Talanta* 129: 594–599.

171 Freitas, M., Nouws, H.P.A., and Delerue-Matos, C. (2019). Electrochemical sensing platforms for HER2-ECD breast cancer biomarker detection. *Electroanalysis* 31: 121–128.

172 Zhao, J., Tang, Y., Cao, Y. et al. (2018). Amplified electrochemical detection of surface biomarker in breast cancer stem cell using self-assembled supramolecular nanocomposites. *Electrochim. Acta* 283: 1072–1078.

173 Gu, C., Guo, C., Li, Z. et al. (2019). Bimetallic ZrHf-based metal-organic framework embedded with carbon dots: ultra-sensitive platform for early diagnosis of HER2 and HER2-overexpressed living cancer cells. *Biosens. Bioelectron.* 134: 8–15.

174 Paimard, G., Shahlaei, M., Moradipour, P. et al. (2019). Impedimetric aptamer based determination of the tumor marker MUC1 by using electrospun core-shell nanofibers. *Mikrochim. Acta* 187: 5.

175 Shahrokhian, S. and Salimian, R. (2018). Ultrasensitive detection of cancer biomarkers using conducting polymer/electrochemically reduced graphene oxide-based biosensor: application toward BRCA1 sensing. *Sens. Actuators, B* 266: 160–169.

176 Majd, S.M., Salimi, A., and Ghasemi, F. (2018). An ultrasensitive detection of miRNA-155 in breast cancer via direct hybridization assay using two-dimensional molybdenum disulfide field-effect transistor biosensor. *Biosens. Bioelectron.* 105: 6–13.

177 Bao, Z., Sun, J., Zhao, X. et al. (2017). Top-down nanofabrication of silicon nanoribbon field effect transistor (Si-NR FET) for carcinoembryonic antigen detection. *Int. J. Nanomed.* 12: 4623–4631.

178 Mostafa, A., Mahdi, R., Navid, N. et al. (2016). An electrochemical nanobiosensor for plasma miRNA-155, based on graphene oxide and gold nanorod, for early detection of breast cancer. *Biosens. Bioelectron.* 77: 99–106.

179 Wang, K., He, M.Q., Zhai, F.H. et al. (2017). A novel electrochemical biosensor based on polyadenine modified aptamer for label-free and ultrasensitive detection of human breast cancer cells. *Talanta* 166: 87–92.

180 Chen, C. and Wang, J. (2020). Optical biosensors: an exhaustive and comprehensive review. *Analyst* 145: 1605–1628.

181 Maya Pai, M., Yallur, B.C., Batakurki, S.R. et al. (2022). Synthesis and catalytic activity of heterogenous hybrid nanocatalyst of copper/palladium MOF, RIT 62-Cu/Pd for Stille polycondensation of thieno[2,3-*b*]pyrrol-5-one derivatives. *Top. Catal.* https://doi.org/10.1007/s11244-022-01618-1.

182 Wang, Y., Wei, Z., Luo, X. et al. (2019). An ultrasensitive homogeneous aptasensor for carcinoembryonic antigen based on upconversion fluorescence resonance energy transfer. *Talanta* 195: 33–39.

183 Mohammadi, S., Mohammadi, S., and Salimi, A. (2021). A 3D hydrogel based on chitosan and carbon dots for sensitive fluorescence detection of microRNA-21 in breast cancer cells. *Talanta* 224: 121895.

184 Bai, Y., Li, H., Xu, J. et al. (2020). Ultrasensitive colorimetric biosensor for BRCA1 mutation based on multiple signal amplification strategy. *Biosens. Bioelectron.* 166: 112424.

185 Choi, J.H., Lim, J., Shin, M. et al. (2021). CRISPR-Cas12a-based nucleic acid amplification-free DNA biosensor via Au nanoparticle-assisted metal-enhanced fluorescence and colorimetric analysis. *Nano Lett.* 21: 693–699.

186 Szymanska, B., Lukaszewski, Z., Hermanowicz-Szamatowicz, K., and Gorodkiewicz, E. (2020). An immunosensor for the determination of carcinoembryonic antigen by surface plasmon resonance imaging. *Anal. Biochem.* 609: 113964.

187 Sina, A.A., Vaidyanathan, R., Wuethrich, A. et al. (2019). Label-free detection of exosomes using a surface plasmon resonance biosensor. *Anal. Bioanal.Chem.* 411: 1311–1318.

188 Wang, Q., Zou, L., Yang, X. et al. (2019). Direct quantification of cancerous exosomes via surface plasmon resonance with dual gold nanoparticle-assisted signal amplification. *Biosens. Bioelectron.* 135: 129–136.

189 Han, Y., Qiang, L., Gao, Y. et al. (2021). Large-area surface-enhanced Raman spectroscopy substrate by hybrid porous GaN with Au/Ag for breast cancer miRNA detection. *Appl. Surf. Sci.* 541: 148456.

190 Wang, H.N., Crawford, B.M., Norton, S.J., and Vo-Dinh, T. (2019). Direct and label-free detection of microRNA cancer biomarkers using SERS-based plasmonic coupling interference (PCI) nanoprobes. *J. Phys. Chem. B* 123: 10245–10251.

191 Wang, H.-M., Wang, A.J., Yuan, P.X., and Feng, J.J. (2020). Flower-like metal-organic framework microsphere as a novel enhanced ECL luminophore to construct the coreactant-free biosensor for ultrasensitive detection of breast cancer 1 gene. *Sens. Actuators, B* 320: 128395.

192 Vinayak, A., Sudha, M., Jagadeesha, A.H. et al. (2014). Synthesis, characterization of some novel 1,3,4-oxadiazole compounds containing 8-hydroxy quinolone moiety as potential antibacterial and anticancer agents. *Int. J. Pharm. Res. 4* (4): 180–185.

193 Cui, A., Zhang, J., Bai, W. et al. (2019). Signal-on electrogenerated chemiluminescence biosensor for ultrasensitive detection of microRNA-21 based on isothermal strand-displacement polymerase reaction and bridge DNA-gold nanoparticles. *Biosens. Bioelectron.* 144: 111664.

194 Adimule, V., Batakurki, S., Yallur, B.C. et al. (2022). Samarium-decorated ZrO_2@ SnO_2 nanostructures, their electrical, optical and enhanced photoluminescence properties. *J. Mater. Sci. – Mater. Electron.* 33: 18699–18715. https://doi.org/10.1007/s10854-022-08718-4.

195 Hartz, J.S.R., Emanetoglu, N.W., Howell, C., and Vetelino, J.F. (2020). Lateral field excited quartz crystal microbalances for biosensing applications. *Biointerphases* 15: 030801.

196 Ramanavicius, S., Jagminas, A., and Ramanavicius, A. (2021). Advances in molecularly imprinted polymers based affinity sensors (review). *Polymers* 13: 974.

197 Gao, Y., Huo, W., Zhang, L. et al. (2019). Multiplex measurement of twelve tumor markers using a GMR multi-biomarker immunoassay biosensor. *Biosens. Bioelectron.* 123: 204–210.

198 Borin, T.F., Arbab, A.S., Gelaleti, G.B. et al. (2016). Melatonin decreases breast cancer metastasis by modulating Rho-associated kinase protein-1 expression. *J. Pineal Res.* 60 (1): 3–15.

199 Li, T., Yang, J., Ali, Z. et al. (2017). Synthesis of aptamer-functionalized Ag nanoclusters for MCF-7 breast cancer cells imaging. *Sci. China Chem.* 60 (3): 370–376.